A low-frequency approximation to the Maxwell equations simultaneously considering inductive and capacitive phenomena

Stephan Koch, Hermann Schneider, and Thomas Weiland
Technische Universität Darmstadt, Institut für Theorie Elektromagnetischer Felder (TEMF)
Schlossgartenstrasse 8, 64289 Darmstadt, Germany
koch/schneider/thomas.weiland@temf.tu-darmstadt.de

***Abstract*—For many technical examples low-frequency approximations to the full set of the Maxwell equations are applicable. Commonly, either the displacement current density or the induced current density are neglected depending on a priori knowledge about the dominating effects for a specific problem setup. This leads to different subsets of the Maxwell equations describing inductive-resistive or capacitive-resistive systems, respectively. Here, a formulation combining both scenarios while maintaining the quasistationary assumption is presented. The formulation is applied to a simple test model consisting of bounded massive conductor embedded in a dielectric insulation.**

I. Introduction

In order to characterize, e.g., the behavior of electrical machines thoroughly, the inclusion of capacitive effects in addition to the inductive ones may become necessary. This situation occurs in particular for inverter-fed electrical machines, where the machine windings are exposed to harmonics caused by the inverter via the connecting cable. The common-mode voltage caused by the inverter in combination with the dielectric insulation of the machine windings gives rise to common-mode currents a higher frequencies [1]. In order to predict these effects, transmission-line models extracted from separate 2D finite element (FE) simulations regarding inductive and capacitive phenomena, respectively, can be applied. Based on the transmission-line parameters, also wave propagation effects in electrical machines can be modeled [2]. Under the assumption of time harmonic excitation functions for the sources of the electromagnetic fields it is straightforward to consider the full set of the Maxwell equations even in the low-frequency regime. Depending on the actual formulation, an instability of the related numerical models resulting from, e.g., a FE discretization is observed if the angular frequency ω tends to zero. This can be resolved by explicitly enforcing Gauss' law as shown in [3]. The singular system matrix resulting from the stabilization can be solved efficiently using appropriate preconditioners as, e.g., the one illustrated in [4].

Neglecting the contribution of the displacement current in the full set of the Maxwell equations leads to the well-known eddy-current formulation. It is valid for sufficiently low frequency under certain restrictions on the material coefficients as well as on the size of the problem domain. This procedure introduces a modeling error which can be estimated as shown in [5], [6]. Due to neglecting the displacement current in the formulation, no electric energy is included in the eddy-current model. This limits the range of application to inductive-resistive systems. Here, an extension in terms of additionally considering capacitive phenomena while remaining in the low-frequency regime is presented.

II. Low-frequency model

Using the magnetic vector potential $\mathbf{A}$ and the electric scalar potential ϕ the ungauged formulation of the Maxwell equations in frequency domain reads

$$\begin{aligned} \nabla \times (\nu \nabla \times \mathbf{A}) + j\omega\sigma\mathbf{A} - \omega^2\varepsilon\mathbf{A} + \\ + (j\omega\varepsilon + \sigma)\nabla\phi = \mathbf{J}_\mathrm{s} \end{aligned} \tag{1}$$

$$\nabla \cdot (\varepsilon \nabla \phi) = \rho \, . \tag{2}$$

Here, the magnetic flux density $\mathbf{B}$ and the electric field strength $\mathbf{E}$ are expressed in terms of the potentials according to $\mathbf{B} = \nabla \times \mathbf{A}$ and $\mathbf{E} = -\nabla\phi - j\omega\mathbf{A}$, respectively. Moreover, ε, σ, $\nu = 1/\mu$ and μ denote permittivity, electric conductivity, reluctivity and permeability. On the righthandside of the above equations, $\mathbf{J}_\mathrm{s}$ and ρ are the source current density and the charge density.

The quasistationary limit is commonly defined based on the relation of diameter d of the domain under consideration and the smallest wavelength λ_min to be expected, see, e.g., [7]. If $d \ll \lambda$ the effects of wave-propagation and radiation are very small. As a consequence, the term $-\omega^2\varepsilon\mathbf{A}$ in (1) can be treated as a small perturbation to the other terms related to the magnetic vector potential [8].

Using the continuity equation while substituting ρ according to Gauss' law while presuming a divergence-free source current density leads to

$$j\omega\nabla\cdot(\sigma\mathbf{A}) - \omega^2\nabla\cdot(\varepsilon\mathbf{A}) + j\omega\nabla\cdot(\varepsilon\nabla\phi) + \nabla\cdot(\sigma\nabla\phi) = 0 \, , \tag{3}$$

which, in the following, is used in the formulation instead of (2) together with (1). In the low-frequency approximation, i.e., $\omega < \omega_\mathrm{max}$ with $\omega_\mathrm{max} = 2\pi c/\lambda_\mathrm{min}$ and c the speed of light, the terms involving ω^2 in (1) and (3) can be dropped accepting the aforementioned modeling error.

Discretizing the modified versions of (1) and (3) by means of lowest order FE edge functions $\mathbf{w}_k$ and nodal shape functions w_i for $\mathbf{A}$ and ϕ, respectively, in combination with Galerkin testing leads to the discrete system

$$\begin{pmatrix} \mathbf{K}_\nu^\mathrm{e} + j\omega\mathbf{M}_\sigma^\mathrm{e} & j\omega\mathbf{L}_\varepsilon^{\mathrm{n,e}} + \mathbf{L}_\sigma^{\mathrm{n,e}} \\ j\omega\left(\mathbf{L}_\sigma^{\mathrm{n,e}}\right)^\mathrm{T} & j\omega\mathbf{K}_\varepsilon^\mathrm{n} + \mathbf{K}_\sigma^\mathrm{n} \end{pmatrix} \begin{pmatrix} \mathbf{a} \\ \mathbf{u} \end{pmatrix} = \begin{pmatrix} \mathbf{j} \\ \mathbf{0} \end{pmatrix} \, . \tag{4}$$

Here, $\mathbf{a}$ and $\mathbf{u}$ are discrete vectors collecting the degrees of freedom for $\mathbf{A}$ and ϕ while $\mathbf{j}$ contains the source current distribution weighted by the test functions $\mathbf{w}_\ell$. The entries of the sub-blocks are defined by

$$\left(\mathbf{K}_\nu^{\mathrm{e}}\right)_{k,\ell} = \int_\Omega (\nabla \times \mathbf{w}_k^{\mathrm{e}}) \cdot \nu \cdot (\nabla \times \mathbf{w}_\ell^{\mathrm{e}}) \, \mathrm{d}V \,, \tag{5}$$

$$\left(\mathbf{M}_\sigma^{\mathrm{e}}\right)_{k,\ell} = \int_\Omega \mathbf{w}_k^{\mathrm{e}} \cdot \sigma \cdot \mathbf{w}_\ell^{\mathrm{e}} \, \mathrm{d}V \,, \tag{6}$$

$$\left(\mathbf{K}_\chi^{\mathrm{n}}\right)_{i,j} = \int_\Omega \nabla w_i^{\mathrm{n}} \cdot \chi \cdot \nabla w_j^{\mathrm{n}} \, \mathrm{d}V \,, \tag{7}$$

$$\left(\mathbf{L}_\chi^{\mathrm{n,e}}\right)_{i,\ell} = \int_\Omega \nabla w_i^{\mathrm{n}} \cdot \chi \cdot \mathbf{w}_\ell^{\mathrm{e}} \, \mathrm{d}V \,, \tag{8}$$

whereas χ is replaced by either ε or σ and Ω denotes the computational domain.

III. System Solution

As no gauging is applied, (4) does not possess a unique solution in terms of the discrete values of the potentials. However, if a numerical solution is found, the resulting fields $\mathbf{B}$ and $\mathbf{E}$ derived from the potentials are unique. Therefore, two different strategies are considered:

1) Solve the complex nonsymmetric system (4) using an appropriate iterative solver.
2) Set the lower left matrix block in (4) to zero and solve the resulting upper triangular block system.

As the righthandside of (4) is divergence-free, the iterative solver (strategy 1) will preserve this property for all iterates up to rounding errors. This effect can be seen as an implicit gauging of the magnetic vector potential [9]. However, in case of large differences in the values of the material coefficients, the severe ill-conditioning might decrease the rate of convergence of the iterative solver significantly. Therefore, an adepted preconditioner should be applied. In case of strategy 2, the solution of (4) can be separated. Given a non-vanishing conductivity in the entire domain leads to a coloumb-like gauge condition and as a consequence the resulting system is regular. The lower right block is then identified as the electroquasistatic system under voltage excitation. Its discrete solution vector $\mathbf{u}$ provides a divergence free current excitation for the magnetoquasistatic system in the upper left block of (4). Therefore, established preconditioners can be used to solve the two smaller systems of equations efficiently.

IV. Test Example

The low-frequency formulation developed above is applied to the test model shown in Fig. 1. A massive conductor ($\sigma = 5 \cdot 10^4\,\mathrm{S/m}$, $\mu_\mathrm{r} = 1000$) is embedded in a block of insulating material ($\varepsilon_\mathrm{r} = 10$). In the surrounding domain as well as for the inferior conductors an artificial conductivity $\sigma_\mathrm{a} = 1 \cdot 10^{-4}\,\mathrm{S/m}$ is assumed. Due to the proximity of the parallel sections of the conductor in combination with the dielectric insulation, capacitive effects become relevant with increasing frequency. In Fig. 2 the amplitude of the current density is illustrated at the center cross-section of the structure. Here, the skin effect dominates while the displacement current is not completely neglected as it is the case for common eddy-current models.

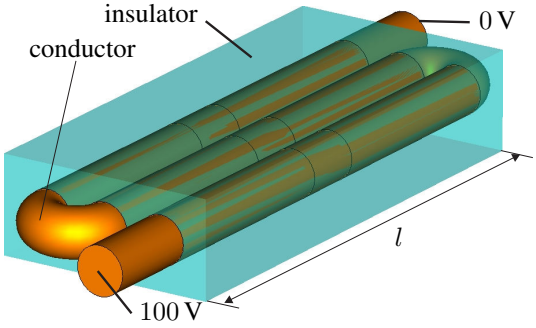

Fig. 1. Example of a bounded massive conductor (diameter $d = 2\,\mathrm{cm}$) embedded in a dielectric material (dimension $l = 20\,\mathrm{cm}$) under a voltage excitation at both ends. The distance in the parallel section is $0.5\,\mathrm{cm}$

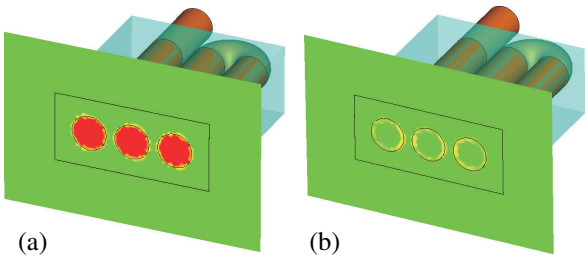

Fig. 2. Qualitative plot of the amplitude of the current distribution at the center cross-section of the massive conductors at (a) $f = 10\,\mathrm{Hz}$ and (b) $f = 1\,\mathrm{MHz}$.

V. Conclusion

Even in the low-frequency approximation of the Maxwell equations it is possible to consider inductive, capacitive and resistive effects in a single model to a certain extent. While the method is used in frequency domain here, the benefit of avoiding the modeling of wave propagation is more obvious in time domain which is favorable, e.g., in presence of nonlinear materials.

References

[1] P. Mäki-Ontto and J. Luomi, "Induction motor model for the analysis of capacitive and induced shaft voltages," in *2005 IEEE International Conference on Electric Machines and Drives*, May 2005, pp. 1653 –1660.

[2] H. De Gersem, O. Henze, T. Weiland, and A. Binder, "Simulation of wave propagation effects in machine windings," *COMPEL: The International Journal for Computation and Mathematics in Electrical and Electronic Engineering*, vol. 29, no. 1, pp. 23–38, 2010.

[3] R. Hiptmair, F. Kramer, and J. Ostrowski, "A robust Maxwell formulation for all frequencies," *IEEE Trans. Magn.*, vol. 44, no. 6, pp. 682–685, Oct. 2008.

[4] J. Ostrowski, M. Bebendorf, R. Hiptmair, and F. Krämer, "$\mathcal{H}$-matrix-based operator preconditioning for full Maxwell at low frequencies," *IEEE Trans. Magn.*, vol. 46, no. 8, pp. 3193–3196, Aug. 2010.

[5] H. Ammari, A. Buffa, and J.-C. Nédélec, "A justification of eddy currents model for the Maxwell equations," *SIAM J. Appl. Math.*, vol. 60, no. 5, pp. 1805–1823, May 2000.

[6] K. Schmidt, O. Sterz, and R. Hiptmair, "Estimating the eddy-current modeling error," *IEEE Trans. Magn.*, vol. 44, no. 6, pp. 686–689, Jun. 2008.

[7] H. K. Dirks, "Quasi-stationary fields for microelectronic applications," *Electr. Eng.*, vol. 79, no. 2, pp. 145–155, Apr. 1996.

[8] B. Doliwa, H. De Gersem, T. Weiland, and T. Boonen, "Optimised electromagnetic 3d field solver for frequencies below the first resonance," *IET Science, Measurement & Technology*, vol. 1, no. 1, pp. 53–56, Jan. 2007.

[9] Z. Ren, "Influence of the RHS on the convergence behaviour of the curl-curl equation," *IEEE Trans. Magn.*, vol. 32, no. 3, pp. 655–658, May 1996.